ELSEVIER

Journal of Alloys and Compounds 467 (2009) 417–423

Journal of ALLOYS AND COMPOUNDS

www.elsevier.com/locate/jallcom

Effect of Te additions on the glass transition and crystallization kinetics of $(Sb_{15}As_{30}Se_{55})_{100-x}Te_x$ amorphous solids

K.A. Aly [a,*], A.A. Othman [b], A.M. Abousehly [a]

[a] *Physics Department, Faculty of Science, Al-Azhar University, Assiut brunch, Assiut, Egypt*
[b] *Physics Department, Faculty of Science, Assiut University, Assiut, Egypt*

Received 18 August 2007; received in revised form 4 December 2007; accepted 6 December 2007
Available online 15 December 2007

Abstract

Differential scanning calorimetry results under non-isothermal conditions of chalcogenide $(Sb_{15}As_{30}Se_{55})_{100-x}Te_x$ (where $0 \leq x \leq 10$ at.%) glasses are reported and discussed. The dependence of the characteristic temperatures "glass transition temperature (T_g), the crystallization onset temperature (T_c) and the crystallization temperature (T_p)" on the heating rate (β) utilized in the determination of the activation energy for the glass transition (E_g), the activation energy for crystallization (E_c), the glass thermal stability ($\Delta T = T_c - T_g$) and the Avrami exponent (n). The composition dependence of the T_g, E_g, and E_c were discussed in terms of the chemical bond approach, the average heats of atomization and the cohesive energy (CE). The diffractogram of the transformed material shows the presence of some crystallites of AsSb, Sb_4Te_6, As_2Se_3 and Sb_2Se_3 in the residual amorphous matrix.

Keywords: Glassy alloy; Non-isothermal process; Heating rate; Glass transition temperature; Crystallization kinetics; Crystalline phases

1. Introduction

Crystallization of chalcogenide glasses plays an important role in determining the transport mechanisms, thermal stability and practical applications [1–4]. The study of crystallization kinetics in amorphous materials by the DSC method has been widely discussed in the literature [5–10]. There are large varieties of theoretical models and functions proposed to explain the crystallization kinetics. The application of each depends on the type of amorphous material studied. In calorimetric measurements, two basic methods can be used, isothermal and non-isothermal method [8,10,11]. In the isothermal method, the sample is brought quickly to a temperature above the temperature of glass transition, T_g and the heat evolved during the crystallization process is recorded as a function of time. In the other method (non-isothermal), the sample is heated at a fixed rate and the heat evolved is again recorded as a function of temperature or time. The isothermal experiments are generally very time-consuming while, experiments performed at constant heating rate are a much more rapid way of studying a transformation. Furthermore, isothermal analysis is the impossibility of reaching a test temperature instantaneously and during the time, which the system needs to stabilize, no measurements are possible while, non-isothermal (constant heating rate) experiments do not have this drawback [8,10].

Tellurium additions to the later glasses would be expected to decrease their glass transition temperature and reduce their thermal stabilities [12]. According to Kastner [13], the addition of an element with a higher electropositive character than the elements in the host material will tend to the decrease of the activation energy for electrical conduction.

The present work study the effect of Te additions on both of the glass transition temperature T_g, the activation energy of glass transition E_g and crystallization kinetics of $(As_{30}Sb_{15}Se_{55})_{1-x}Te_x$ ($x = 0$, 2.5, 7.5, and 10 at.%) glasses.

2. Theoretical background

The theoretical bases for interpreting DTA or DSC results is provided by the formula theory of transformation kinetics as the volume fraction (χ) crystallized in time (t) by using the Johnson,

* Corresponding author.
E-mail address: Kamalaly2001@yahoo.com (K.A. Aly).

0925-8388/$ – see front matter © 2007 Elsevier B.V. All rights reserved.
doi:10.1016/j.jallcom.2007.12.009

Mehl and Avrami's equation [14].

$$\chi = 1 - \exp(-(kt)^n) \tag{1}$$

where n is an integer or half integer depends on the mechanism of growth and the dimensionality of the crystal, k is defined as the effective (overall) reaction rate, which is usually assumed to have an Arrhenian temperature dependence.

$$k = k_0 \exp\left(\frac{-E}{RT}\right) \tag{2}$$

where E is the effective activation energy describing the overall crystallization process.

2.1. Bansal's method

In a non-isothermal DSC experiment the rate constant K, changes continually with time due to the change of the temperature and Eq. (1) can be rewritten in the form [15]

$$\chi(t) = 1 - \exp\left[-\left(\int_0^t K[T(\bar{t})]\,\mathrm{d}\bar{t}\right)^n\right] = 1 - \exp(-I^n) \tag{3}$$

Deriving Eq. (3) with respect to time, the crystallization rate is obtained as

$$\dot{\chi} = nK(1-\chi)I^{n-1} \tag{4}$$

The maximum rate of crystallization occurs at the peak of the exotherm at time t_p and temperature T_p [14], the differentiation of Eq. (4) with respect to time yields

$$\ddot{\chi} = nK_p(I^n)_p - (n-1)K_p - \frac{\beta E I_p}{RT_p^2} = 0 \tag{5}$$

The time integral in Eq. (3) is transformed to temperature integral yielding

$$I(T) = \frac{K_0}{\alpha}\int_{T_0}^{T} \exp\frac{-E}{R\bar{T}}\,\mathrm{d}\bar{T} \tag{6}$$

which is represented by several approximate analytical expressions [16–19] by the sum of the alternating series

$$S(\bar{y}) = \frac{\mathrm{e}^{-\bar{y}}}{\bar{y}^2}\sum_{k=0}^{k=\infty}\frac{(-1)^k(k+1)!}{\bar{y}^k} \tag{7}$$

where $\bar{y} = E/R\bar{T}$. Considering that, in this type of series the error produced is this less than the first term neglected and bearing in mind that, in most crystallization reactions $\bar{y} = E/R\bar{T} \gg 1$, it possible to use only the two first terms of this series and the error introduced is not greater than 1%. By assuming that,

$$T^2(1-2RT/E)\exp(-E/RT) \gg T_0^2(1-2RT_0/\bar{E})\exp(-E/RT_0)$$

Eq. (6) becomes

$$I = K_0E(\beta R)^{-1}\mathrm{e}^{-y}y^{-2}(1-2y^{-1}) \tag{8}$$

considering the assumptions used to get Eq. (8) and taking the logarithm of the quoted equation leads to an expression that in the range of values of $y = E/RT$, $25 \le y \le 55$, can be fitted very satisfactorily by a linear approximation (an additional assumption) yielding [20]

$$\ln[\mathrm{e}^{-y}y^{-2}(1-2y^{-1})] \cong -5.304 - 1.052y \tag{9}$$

Substituting into Eq. (8)

$$I = K_0E(\beta R)^{-1}\exp(-5.304 - 1.052y) \tag{10}$$

where the above-mentioned approximation might introduce 5.8% error in the value of $\mathrm{e}^{-y}y^{-2}(1-2y^{-1})$ in the worst cases.

Substituting for ($y = E/RT$) and ($K = K_0\exp(-E/RT)$) into Eq. (10) gives

$$I = RT^2K(\beta E)^{-1}\left(\frac{1-2RT}{E}\right) \tag{11}$$

if it is assumed that $T \gg T_0$ so that, y_0 can be taken as infinity, the last expression of the integral I is

$$I_p = \left(\frac{1-2RT_p}{nE}\right)^{1/n} \tag{12}$$

Substituting for I into Eq. (5) and taking the logarithmic form

$$\ln\left(\frac{T_p^2}{\beta}\right) + \ln\left(\frac{K_0R}{E}\right) - \frac{E}{RT_p} \approx \left(\frac{2RT_p}{E}\right)\left(\frac{1-1}{n^2}\right) \tag{13}$$

note that, Eq. (13) reduces to the Kissinger's expression [6] for the case of $n = 1$ as one might have anticipated since this corresponds to the homogeneous reaction case. Thus, it can be seen that, the Kissinger's method is appropriate for the analysis not only for homogeneous reactions, but also for the analysis of heterogeneous reactions which are described by the JMA equation in the isothermal experiments [14]. The approximation in Eq. (13) RHS = 0 yielding,

$$\ln\left(\frac{T_p^2}{\beta}\right) = \frac{-E_c}{RT_p} - \ln\left(\frac{K_0R}{E}\right) \tag{14}$$

where the quoted approximation might introduce a 3% error in the value of E/R in the worst cases.

Finally, it should be noted that, the term $(-2RT/E)$ in Eq. (11) is negligible in comparison to the unity, since in most crystallization reactions $E/RT \gg 25$ [14]. Therefore, Eq. (11) may be rewritten

$$I = RT^2K(\beta E)^{-1} \tag{15}$$

Substituting for I into Eq. (4) gives

$$\dot{\chi}_p = \frac{n(0.37\beta E_c)}{(RT_p^2)} \tag{16}$$

That makes it possible to calculate kinetic exponent n.

2.2. Matusita's method

This theory describes the evolution with time, t, of the volume fraction crystallized, χ, by Eq. (3) according to the formula theory of transformation kinetics using the Johnson–Mehl and

Avrami equation [14]. Taking the logarithm of Eq. (3) and substituting Eq. (8) one obtains

$$-\ln(1-\chi) = C_0\beta^{-n}\exp\left(-\frac{1.025mE}{RT}\right) \quad (17)$$

where $n = m+1$ for a quenched glass containing no nuclei and $n = m$ for a glass containing sufficiently large number of nuclei, taking the logarithmic form of Eq. (17) yields [20].

$$\ln[-\ln(1-\chi)] = -n\ln\beta - 1.052\left(\frac{mE_c}{RT}\right) + \text{const.} \quad (18)$$

The slope of the linear relation between $\ln[-\ln(1-\chi)]$ and $\ln(\beta)$ represents the value of the kinetic exponent (n) and the effective activation energy E can be determined from the relation between $\ln[-\ln(1-\chi)]$ and $1/T$.

3. Experimental details

The semiconducting $(Sb_{15}As_{30}Se_{55})_{100-x}Te_x$ (with $x = 0$, 2.5, 7.5 and 10 at.%) chalcogenide glasses was prepared from their high purity (99.999%) components. The proper amount for each material was weighed and introduced into cleaned silica tubes. To avoid the oxidation of the samples the tube was evacuated to 1.33×10^{-3} Pa, then put into a furnace at around 1250 K for 24 h. During the course of heating the ampoule was shaken several times to maintain their uniformity. Finally, the ampoule was quenched into ice cooled water to avoid crystallization.

The amorphous state of the material was confirmed by a diffractometric X-ray scan (Philips diffractometer 1710) using Cu as target and Ni as filter ($\lambda = 1.542$ Å). Energy dispersive X-ray spectroscopy (link analytical EDS) was used to measure the elemental composition and indicates that the investigated composition is correct up to ±0.2 at.%.

The calorimetric measurements were carried out using differential scanning calorimeter Shimadzu 50 with an accuracy of 0.1 K, keeping a constant flow of nitrogen to extract the gases generated during the crystallization reactions, which, is a characteristic of chalcogenide materials. The calorimeter was calibrated, for each heating rate, using the well-known melting temperatures and melting enthalpies of zinc and indium supplied with the instrument [21,22]. 20 mg powdered samples, crimped into aluminium pans and scanned at continuous heating rates ($\beta = 2.5$, 5, 10, 15, 20, 25 and 30 K min^{-1}). The value of the glass transition temperature, T_g, the crystallization extrapolated onset, T_c, and the crystallization peak temperature, T_p, were determined with accuracy ±1 K by using the microprocessor of the thermal analyzer.

The fraction, χ, crystallized at a given temperature, T, is given by $\chi = A_T/A$, where A is the total area of the exotherm between the temperature, T_i, where crystallization is just beginning and temperature, T_f, where the crystallization is completed, A_T is the area between T_i and T, as shown in Fig. 1.

4. Results and discussion

Fig. 2 shows a set of DSC thermogram for different compositions of the $(Sb_{15}As_{30}Se_{55})_{100-x}Te_x$ glasses recorded at heating rates 10 K/min. This figure shows that, both of the characteristic temperatures, T_g, T_c and T_p decreases with the increase in Te content. Also, it can be note that, the thermal stability ($\Delta T = T_c - T_g$) of these glasses decreases with the increase in Te content. See Table 1.

4.1. Glass transition

Two approaches were used to analyze the dependence of glass transition temperature on the heating rate (β). The first is the

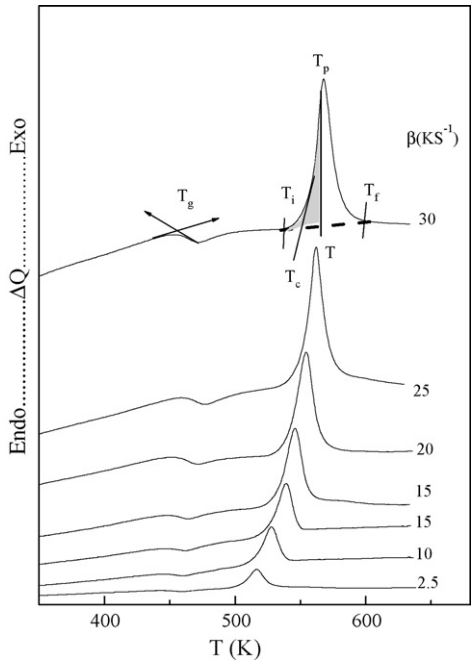

Fig. 1. DSC traces for powdered $(Sb_{15}As_{30}Se_{55})_{92.5}Te_{7.5}$ chalcogenide glass at different heating rates. The hatched area shows A_T, the area between T_i and T.

empirical relationship that can be written in the following form

$$T_g = A + B\ln b \quad (19)$$

where A and B are constants for a given glass composition [23].The results shown in Fig. 3 indicate the validity of Eq. (19) for the $(As_{30}Sb_{15}Se_{55})_{1-x}Te_x$ glasses.

The second approach is the dependence of the glass transition temperature on the heating rate, β, by using Kissinger's formula [6] in the form

$$\ln\left(\frac{T_g^2}{\beta}\right) = \frac{-E_c}{RT_g} + \text{const.} \quad (20)$$

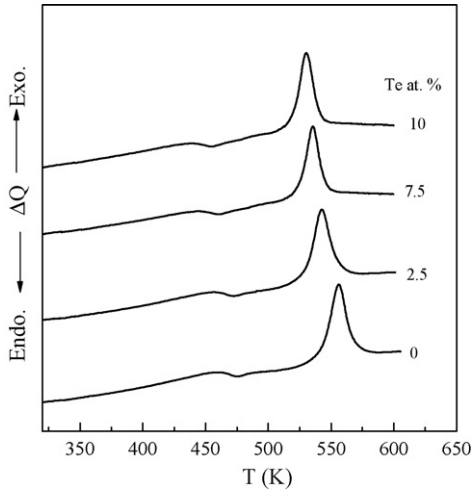

Fig. 2. DSC thermograms of $(As_{30}Sb_{15}Se_{55})_{1-x}Te_x$ glasses recorded at heating rate 10 K/min.

Table 1
The dependence of the glass transition temperature T_g, the thermal stability ($\Delta T = T_c - T_g$), and the activation energy of glass transition E_g (kJ mol^{-1}) on the Te content of $(As_{30}Sb_{15}Se_{55})_{1-x}$ Te$_x$ glasses

Te (at.%)	T_g (K)	ΔT (K)	E_g (Eq. (18))	E_g (Eq. (19))	$\langle E_g \rangle$
0	462.52	79.92	298.08	305.93	302.01
2.5	454.92	78.44	293.8	300.32	297.05
7.5	436.05	63.38	285.21	292.47	288.84
10	432.14	66.98	283.56	285.99	284.78

A straight line between $\ln(T_g^2/\beta)$ and $1/T_g$, whose slope yields a value of E_g, given that, the variation of $\ln(T_g^2)$ with β is negligibly small compared with the variation of $\ln(\beta)$, it is possible to write [23,5].

$$\ln(\beta) = \frac{-E_g}{RT_g} + \text{const.} \quad (21)$$

Fig. 4(a) shows plots of $\ln(T_g^2/\beta)$ and (b) $\ln(\beta)$ (versus $1/T_g$ for different compositions of $(As_{30}Sb_{15}Se_{55})_{1-x}Te_x$ chalcogenide glasses, displaying the linearity of the used equations. The obtained values of the glass transition activation energy E_g are listed in Table 1.

The deduced values of E_g lie within the observed values for chalcogenide glasses [5,24,25]. The observed decrease of E_g with increasing Te content resulted in an apparent decrease of T_g with increasing Te content. These results are in good agreement with those obtained by Cofmenero and Barandiaran [26]. Therefore, the rigidity of glasses decreases with increasing Te content. The glass transition temperature is known to depend on several independent parameters such as the band gap, bond energy, effective molecular weight, the type and fraction of various structural units formed and the average coordination number [27,28]. Ioffe and Regal [29] suggested that, the bonding character in the nearest-neighbor region, which means the coordination number N_r, characterizes the electronic properties of semiconducting materials; the average coordination number N_r of $As_aSb_bSe_cTe_d$ glasses can be expressed as

$$N_r(\text{AsSbSeTe}) = \frac{a.N_r\text{As} + b.N_r\text{Sb} + c.N_r\text{Se} + d.N_r\text{Te}}{a+b+c+d} \quad (22)$$

Determination of N_r allows the estimation of the number of constraints N_s. This parameter is closely related to the glass-transition temperature and its related properties. For a material with coordination number N_r, N_s can be expressed as the sum of the radial and angular valence force constraints [30],

$$N_s = \frac{N_r}{2} + (2N_r - 3) \quad (23)$$

The calculated values for N_r and N_s of the $(As_{30}Sb_{15}Se_{55})_{1-x}Te_x$ system are listed in Table 3 using the values of N_r for As, Se, Sb and Te [31] that are given in Table 2. One can be observed that, both of the N_r and N_s decreases with increasing Te content. In a covalently bonded glass network two types of constraints, bond bending N^γ and bond stretching N^α need to be counted. For an atomic species with coordination number N_r, the number of constraints per atom arising from bond bending is $N^\gamma = 2N_r - 3$ and from bond stretching is $N^\alpha = N_r/2$. Thus, the addition of Te reduces the number of constraints per atom.

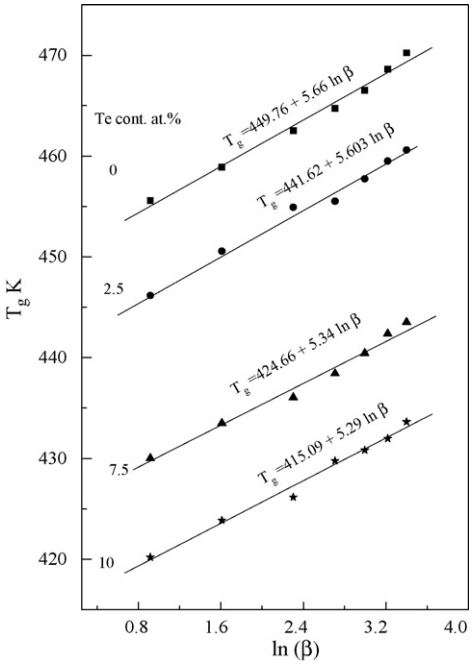

Fig. 3. Glass transition temperature T_g versus $\ln(\beta)$ for $(As_{30}Sb_{15}Se_{55})_{1-x}Te_x$ ($x = 0$, 2.5, 7.5 and 10 at.%) chalcogenide glasses.

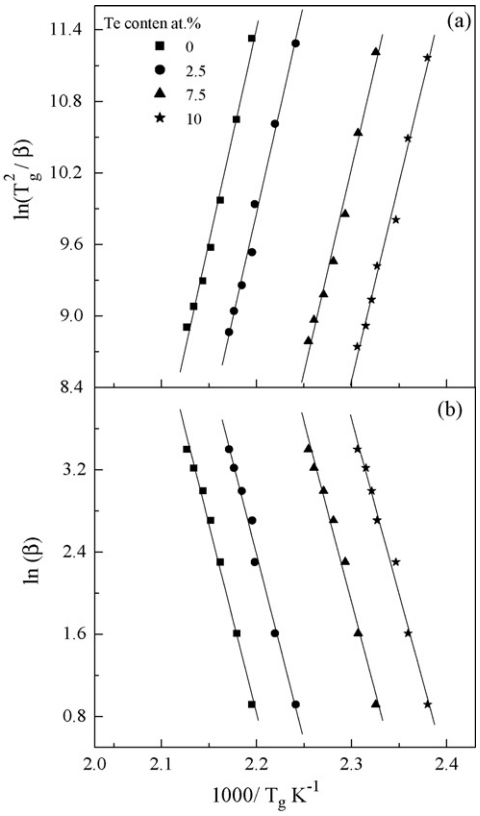

Fig. 4. (a) $\ln(T_g^2/\beta)$ versus $1/T_g$ and (b) $\ln(\beta)$ versus $1/T_g$ for $(As_{30}Sb_{15}Se_{55})_{1-x}Te_x$ chalcogenide glasses.

Table 2
Some of the physical properties and electronic structure of As, Se, Sb and Te atoms

Property	As	Se	Sb	Te
Coordination number [31]	3	2	3	2
H_s (kcal g atom^{-1}) [33]	69.0	49.4	62.0	46
Electronegativity [38]	2.18	2.55	2.05	2.1
Bond energy (kJ mol^{-1}) [37]	32.10	44.04	30.22	33

According to Pauling [32], the heat of atomization $H_s(A-B)$, at standard temperature and pressure of a binary semiconductor formed from atoms A and B, is the sum of the heat of formation ΔH and the average of the heats of atomization H_s^A and H_s^B that corresponds to, the average non-polar bond energy of the two atoms

$$H_s(A-B) = \Delta H + \tfrac{1}{2}(H_s^A + H_s^B) \quad (24)$$

The first term in Eq. (24) is proportional to the square of the difference between the electro negativities χ_A and χ_B of the two atoms

$$\Delta H\alpha(\chi_A - \chi_B)^2$$

This idea can be extended to quaternary semiconductor compounds according to Sadagopan and Gotos [33]. In most cases, the heat of formation of chalcogenide glasses is unknown. In the few materials for which it is known, its value does not exceed 10% of the heat of atomization and therefore can be neglected [34,35]. Hence, $H_s(A-B)$ is given quite well by

$$H_s(A-B) = \tfrac{1}{2}(H_s^A + H_s^B) \quad (25)$$

The obtained results of the heat of atomization of $(As_{30}Sb_{15}Se_{55})_{1-x}Te_x$ (where $x=0$, 2.5, 5, 7.5, 10 and 12.5 at.%) glasses are listed in Table 3, using the values of H_s for As, Se, Sb and Te given in Table 2.

The bond energies $D(A-B)$ for hetero-nuclear bonds have been calculated by using the empirical relation proposed by Pauling [36] as

$$D(A-B) = [D(A-A)\cdot D(B-B)]^{1/2} + 30(\chi_A - \chi_B)^2 \quad (26)$$

where $D(A-A)$and $D(B-B)$ are the energies of the homo-nuclear bonds (in units kcal mol^{-1}) [37], χ_A and χ_B are the electro negativity values for the involved atoms [38]. Bonds are formed in the sequence of decreasing bond energy until the available valence of atoms is satisfied [39]. In the present compositions, the Se–Te bonds with the highest possible energy

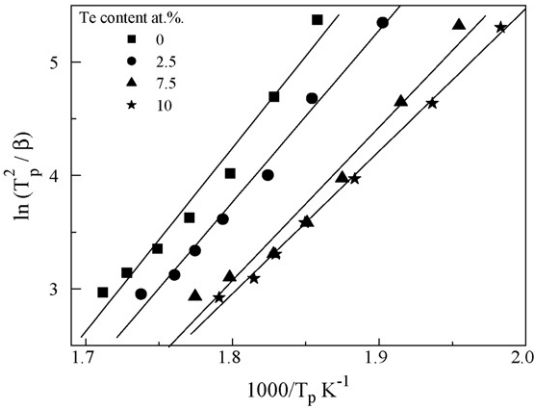

Fig. 5. $\ln(T_g^2/\beta)$ versus $1/T_p$ for $(As_{30}Sb_{15}Se_{55})_{1-x}Te_x$ chalcogenide glasses.

(44.20 kcal mol^{-1}) are expected to occur first. Since the Sb–Se (43.98 kcal mol^{-1}) followed by As–Se (41.71 kcal mol^{-1}) to saturate all available valence of Se. There are still unsatisfied as which must be satisfied by As–As defect homo-polar bonds. Based on the chemical bond approach, the bond energies are assumed to be additive. Thus, the cohesive energies were estimated by summing the bond energies over all the bonds expected in the material. Calculated values of the cohesive energies for all compositions are presented in Table 3. These results indicate that, the cohesive energies of these glasses show a decrease with increasing Te content. Therefore, it can be concluded that the decrease of E_g with increasing Te content is most probably due to the reduction of the average stabilization energy by Te content. It should be mentioned that the approach of the chemical bond neglects dangling bond and other valence defects as a first approximation. Also van der Walls interactions are neglected, which can provide a means for further stabilization by the formation of much weaker links than regular covalent bonds.

4.2. Crystallization

For the evaluation of activation energy for crystallization (E_c) and the frequency factor K_0 from the variation of T_p with β one can use Eq. (14) [15]. The plot of $\ln[T_p^2/\beta]$ versus $1/T_p$ is shown in Fig. 5.

The area under the DSC curve is directly proportional to the total amount of the alloy crystallized. The ratio between the ordinates and the total area of the peak gives the corresponding crystallization rates, which make it possible, to plot the curves of the exothermal peaks represented in Fig. 6. It may be observed

Table 3
The calculated values of the average coordination number N_r, the number of constraints N_s (N + N), the average heat of atomization H_s, the excess of As—As bonds and the cohesive energy CE for the investigated $(As_{30}Sb_{15}Se_{55})_{1-x}Te_x$ system with ($x=0$, 2.5, 7.5 and 10 at.%)

Te cont. (at.%)	N_r	N_s	N^α	N^γ	H_s (kcal g atom^{-1})	Excess As—As	CE (eV atom^{-1})
0	2.45	3.125	1.225	1.9	57.17	26	2.205
2.5	2.439	3.097	1.219	1.877	56.89	30	2.184
7.5	2.416	3.041	1.208	1.833	56.33	38	2.158
10	2.405	3.013	1.203	1.81	56.05	42	2.135

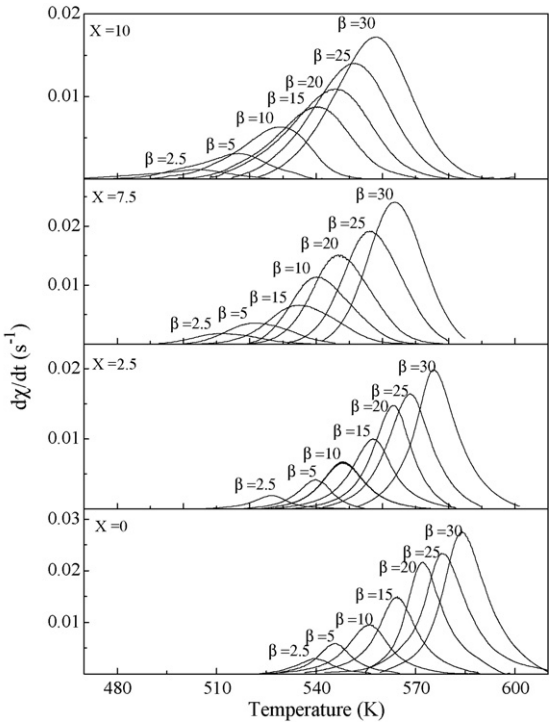

Fig. 6. Crystallization rate versus temperature of the exothermal peaks at different heating rates for different compositions of $(As_{30}Sb_{15}Se_{55})_{100-x}Te_x$ chalcogenide glasses.

that, the $(d\chi/dt)_p$ values increases as well as the heating rate, a property which has been widely discussed in the literature [40].

With the aim of the correct applying of the preceding theory, the materials were reheated up to a temperature slightly higher than T_g) for 1 h in order to form a large number of nuclei. It was ascertained by X-ray diffraction that, there is no crystalline peaks were detected after the nucleation treatment while there are some crystalline peaks observed after annealing the $(As_{30}Sb_{15}Se_{55})_{92.5}Te_{7.5}$ glass at 534 K ($>T_p$) for 2 h. The diffractogram of the transformed material after heat treatment Fig. 7 suggests the presence of some crystallites of AsSb, Sb_4Te_6, As_2Se_3 and Sb_2Se_3 indicated with d and I, respectively, while there remain also a residual amorphous phase.

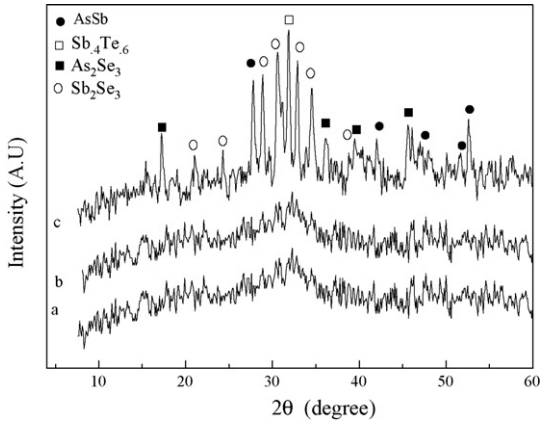

Fig. 7. (a) X-ray diffraction pattern for $(As_{30}Sb_{15}Se_{55})_{92.5}Te_{7.5}$ glass (a) as prepared, (b) annealed at 400 K, and (c) annealed at T_p for 2 h.

From the experimental data, It has been observed that, the correlation coefficients of the corresponding straight regression lines show a maximum value for a given temperature, which was considered as the most adequate one for the calculation of parameter n by using Eq. (16). It was found that, the n value for the as-quenched glass very close to that for the reheated glass. Allowing to experimental error, both values are close to each other. This indicates that, a large number of nuclei exist already in the material, and therefore $m = n$ for all glasses under study. It was found that, $n = m = 3$ for $(As_{30}Sb_{15}Se_{55})_{100-x}Te_x$ glasses with $x = 0$, 7.5 while, $n = m = 2$ for $(As_{30}Sb_{15}Se_{55})_{100-x}Te_x$ glasses with $x = 2.5$, 10 glasses. In addition, $n = m + 1$ for as-quenched glass containing no nuclei while $n = m$ for a glass containing a sufficiently large number of nuclei. The kinetic parameters were deduced based on the mechanism of crystallization. The value of the kinetic exponent ($n = 2$) for the as-quenched glass is consistent with the mechanism of volume nucleation with one dimensional growth and the value of the kinetic exponent ($n = 3$) is consistent with the mechanism of volume nucleation with two dimensional growth.

Finally, the crystallization activation energy, E_c, can be deduced using the formula (Eq. (14)) suggested by Matusita et al. [20]. When $\ln[-\ln(1-\chi)]$ is plotted versus $1/T_p$ a straight line is obtained whose slope is $[(1.052mE_c)/R]$ as shown in Fig. 8. The deduced E_c values according to Ref. [20] for $(As_{30}Sb_{15}Se_{55})_{100-x}Te_x$ glasses were listed in Table 4. From this table we can notice the activation energy of crystallization decreases with increasing Te content these results in good agreement with those obtained by Wahab and Fayek [41]. They found

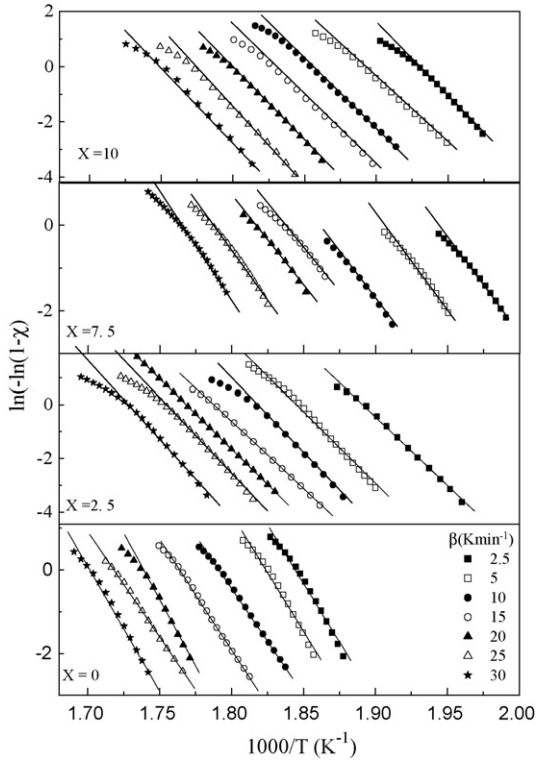

Fig. 8. $\ln[-\ln(1-x)]$ versus $1/T$ plots calculated from the exothermic peaks at different heating rates for $(As_{30}Sb_{15}Se_{55})_{1-x}Te_x$ glasses.

Table 4
The dependence of the activation energy of glass transition E_c (kJ mol^{-1}), the frequency factor K_0 and the Avrami's exponent on the Te content of $(As_{30}Sb_{15}Se_{55})_{1-x}Te_x$ glasses

Te (at.%)	E_c (Eq. (14))	K_0 (10^7 s^{-1}) (Eq. (14))	$\langle n \rangle$ (Eq. (16))	E_c (Eq. (18))
0	134.58	298.08	3	144.27
2.5	125.98	293.8	2	134.16
7.5	112.43	285.21	3	113.77
10	104.51	283.56	2	110.1

that the addition of Te onto AsSe glasses reduce their activation energy of crystallization that means that, the addition of Te assists the crystallization.

5. Conclusion

The addition of Te at the expense of Se, As (Sb) of $(Sb_{15}As_{30}Se_{55})_{100-x}Te_x$ chalcogenide glasses result in:

1. The decrease of characteristic temperatures (T_g, T_c, and T_p) that leads to the decrease of both of the activation energy of glass transition E_g and crystallization E_c.
2. The obtained results well discussed in terms of the coordination number, the chemical bond approach, the average heats of atomization and the cohesive energy CE.
3. The numerical factors, n and m depend on the mechanism of nucleation, growth, and the dimensionality of the crystal. In addition, $n = m + 1$ for as-quenched glass containing no nuclei while $n = m$ for a glass containing a sufficiently large number of nuclei. The kinetic parameters were deduced based on the mechanism of crystallization. The value of the kinetic exponent ($n = m = 2$) for the as-quenched glass is consistent with the mechanism of volume nucleation with one dimensional growth and the values ($n = m = 3$) is consistent with the mechanism of volume nucleation with two dimensional growth.
4. Finally, the identification of the crystalline phases reveals the existence of some crystallites of AsSb, Sb_4Te_6, As_2Se_3 and Sb_2Se_3 dispersed in the remaining amorphous matrix.

References

[1] N. Afify, J. Non-Cryst. Solids 142 (1992) 247.
[2] N. Afify, J. Non-Cryst. Solids 136 (1991) 67.
[3] A.K. Agnihotri, A. Kumar, A.N. Nigam, J. Non-Cryst. Solids 101 (1988) 127.
[4] V. Damodara Das, P. Jansi Lakshmi, Phys. Rev. B 37 (1988) 720.
[5] S. Mahadevan, A. Giridhar, A.K. Singh, J. Non-Cryst. Solids 88 (1986) 11.
[6] H.E. Kissinger, Anal. Chem. 29 (1957) 1702.
[7] M.A. Abdel-Rahim, M. Abu El-Oyoun, A.A. Abu-Sehly, J. Phys. D: Appl. Phys. 34 (2001) 2541.
[8] J. Vazquez, P.L. Lopez-Alemany, P. Villares, R. Jimenez-Garay, J. Phys. Chem. Solids 61 (2000) 493.
[9] A.A. Othman, K.A. Aly, A.M. Abousehly, phys. status solidi (a) 203-5 (2006) 837.
[10] M.J. Strink, A.M. Zahra, Thermochim. Acta 298 (1997) 179.
[11] A. El-Salam, M. Abousehly, J. Therm. Anal. 46 (1996) 177.
[12] J.A. Savage, J. Non-Cryst. Solids 47 (1) (1982) 101–116.
[13] M. Kastner, Phys. Rev. Lett. 28 (1972) 355.
[14] W.A. Johnson, K.F. Mehl, Trans. Am. Inst. Min. Eng. 135 (1981) 315.
[15] N.P. Bansal, R.H. Doremus, A.J. Bruce, C.T. Moynihan, J. Am. Ceram. Soc. 66 (1983) 233.
[16] M. Abramowitz, I.E. Stegun, Handbook of Mathematical Functions, Dover, New York, 1972.
[17] I.S. Gradshteyn, I.M. Ryzhik, Table of Integrals, Series and Products, Academic Press, New York, 1980.
[18] C.D. Doyle, Nature 207 (1965) 290.
[19] J. Vazquez, C. Wagner, P. Villares, R. Jimenez-Garay, Acta Mater. 44 (1996) 4807.
[20] K. Matusita, T. Konatsu, R. Yorota, J. Mater. Sci. 19 (1984) 291.
[21] Perkin Elmer, PC Series, Thermal Analysis System, DSC 7 Di.erential Scanning Calorimeter, OperatorÕs Manual, Norwalk, Connecticut, 1989.
[22] G.W.H. Höhne, W. Hemminger, H.-J. Flammershiem, Differential Scanning Calorimetry, Springer-Verlag, Berlin, Heidelberg, 1996.
[23] A.A. Othman, K.A. Aly, A.M. Abousehly, Solid State Commun. 138 (2006) 184–189.
[24] M.A. Abdel-Rahim, J. Non-Cryst. Solids 241 (1998) 121–127.
[25] R.A. Ligero, J. Vazquez, P. Villares, R. Jimenze-Garay, Thermochim. Acta 157 (1990) 181.
[26] J. Cofmenero, J.M. Barandiaran, J. Non-Cryst. Solids 30 (1979) 263.
[27] A. Giridhar, S. Mahadevan, J. Non-Cryst. Solids 151 (1992) 245.
[28] M.K. Rabinal, K.S. Sangunni, E.S.R. Gopal, J. Non-Cryst. Solids 188 (1995) 98.
[29] A.F. Ioffe, A.R. Regel, Prog. Semicond. 4 (1960) 239.
[30] J.C. Phillips, M.F. Thorpe, Solid State Commun. 53 (1985) 699.
[31] L. Tichy, H. Ticha, J. Non-Cryst. Solids 189 (1995) 141.
[32] L. Pauling, J. Phys. Chem. 58 (1954) 662.
[33] V. Sadagopan, H.C. Gotos, Solid State Electron. 8 (1965) 529.
[34] S.S. Fouad, Vacuum 52 (1999) 505.
[35] S.S. Fouad, A.H. Ammar, M. Abo-Ghazala, Physica B 229 (1997) 249.
[36] J. Pauling, Nature of the Chemical Bond Ithaca, Cornell University Press, NY, 1960.
[37] L. Tichy, A. Triska, H. Ticha, M. Frumar, J. Klikorka, Solid State Commun. 41 (1982) 751.
[38] J. Bicermo, S.R. Ovshinsky, J. Non-Cryst. Solids 74 (1985) 75.
[39] B. Jozef, O. Stanford, S. Mahadevan, A. Gridhar, A.K. Singh, J. Non-Cryst. Solids 74 (1985) 75.
[40] P.L. Lopez-Alemany, J. Vazquez, P. Villares, R. Jimenez-Garay, J. Alloys Compd. 285 (1999) 185–193.
[41] L.A. Wahab, S.A. Fayek, Solid State Commun. 100-5 (1996) 345–350.